REAL TIME VISUALIZATION AND PREDICTION OF SOLDER PASTE FLOW IN THE CIRCUIT BOARD PRINT OPERATION

Dr. Gerald Pham-Van-Diep, Srinivasa Aravamudhan, and Frank Andres
Cookson Electronics, Equipment Group
Franklin, MA

ABSTRACT

Three studies are undertaken to understand the dependence of aperture fill and stencil release on solder paste print definition. The first study focuses on the role of pastes. Seven pastes are compared and ranked by release performance. Second, three stencil-forming techniques are compared. Chemical etch, laser machined and electro-formed stencils from two manufacturers are studied to determine critical design parameters. Third, a model describing the release mechanism including sheer and adhesion forces is developed and compared to experimental results. Additionally, a real-time visualization technique and a model for solder paste flow into stencil apertures during the squeegee operation are described and results discussed.

Key words: surface mount, fine feature, transfer efficiencies, solder paste, stencil printing.

INTRODUCTION

Because stencil printing is not well understood, it is the source of the majority of defects encountered in the printed circuit board (PCB) assembly process [1]. A better understanding of the basic principles involved in the stencil printing operation would enable increased yields for current, as well as, small scale print features.

This paper describes a real time visualization technique developed to study aperture fill and stencil release of the solder print operation. This is accomplished by viewing both processes in real time by means of a high-speed camera, magnifying lens, and careful lighting/optical access combination. This unique method allows for a rapid qualitative analysis, while at the same time eliminating sources of error associated with typical post-print measurement systems. It also allows a real time observation of the paste dynamics and surface effects involved in the printing operation, and thus enables interpretation of the mechanisms governing the release process.

REAL TIME VISUALIZATION OF THE RELEASE PROCESS

Visualization Tool

Central to the work described in this paper is a real time visualization tool capable of simultaneously imaging the stencil and the substrate while separation occurs. The visualization technique has been borrowed from work previously done on examining the release efficiency of various small apertures and shapes [2]. A schematic of the setup is illustrated in Figure 1.

A high-speed camera equipped with a telescope has been used in this study. Careful design of the experiment allowed for direct optical access to the space between the stencil and the substrate. Since this space grows from nil to about twice the stencil thickness during a release, lighting is critical for reliable imaging. It can be seen from examples provided in Figures 3-7 that as the space between the stencil and the substrate increases, so does the amount of light in the frame. Since the camera exposure time is fixed, the frames in the release sequences become brighter as the stencil/substrate gap increases. The camera was operated at 250 frames/sec with a 512 X 480 active pixel array. A relative separation velocity of 0.1 in./sec was chosen for the experiments presented in this study. The selected substrate was initially BK7 glass but was later switched to bare copper.

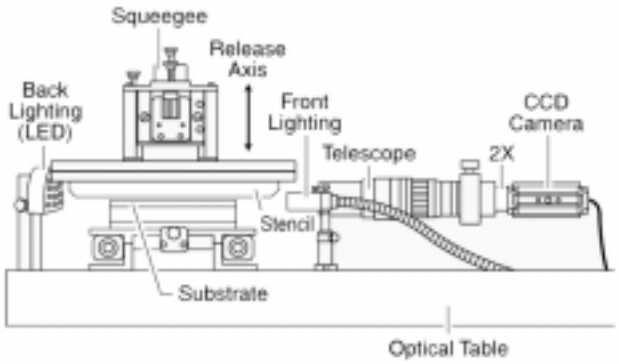

Figure 1: Schematic of real time print dynamics visualization platform.

Ranking Technique

In order to compare two experimental conditions, the release performance of two pastes for example, a series of four release sequences were acquired for each experiment. For the sake of argument we shall call the sequences corresponding to experiment A: (A1...A4) and the sequences corresponding to experiment B: (B1...B4). Each sequence from series A was compared to each sequence of series B: A1 vs. B1, A1 vs. B2, etc. For each comparison pair, a score was assigned solely on the basis of whether Ai released better than Bj (+1 for better, -1 for worse, 0 for equal performance).

The sum for all pairs of possible and non-repeating Ai and Bj combinations was then computed to arrive at the final score of experiment A versus B. Hence, the maximum score one paste can achieve versus another is 16 (minimum: -16). If multiple pastes are to be compared, the sum for all scores are added for each paste comparison, ultimately yielding a relative score for all pastes compared. A chart of the scoring procedure is shown in Figure 2, where two pastes are compared to each other on the basis of their release performance.

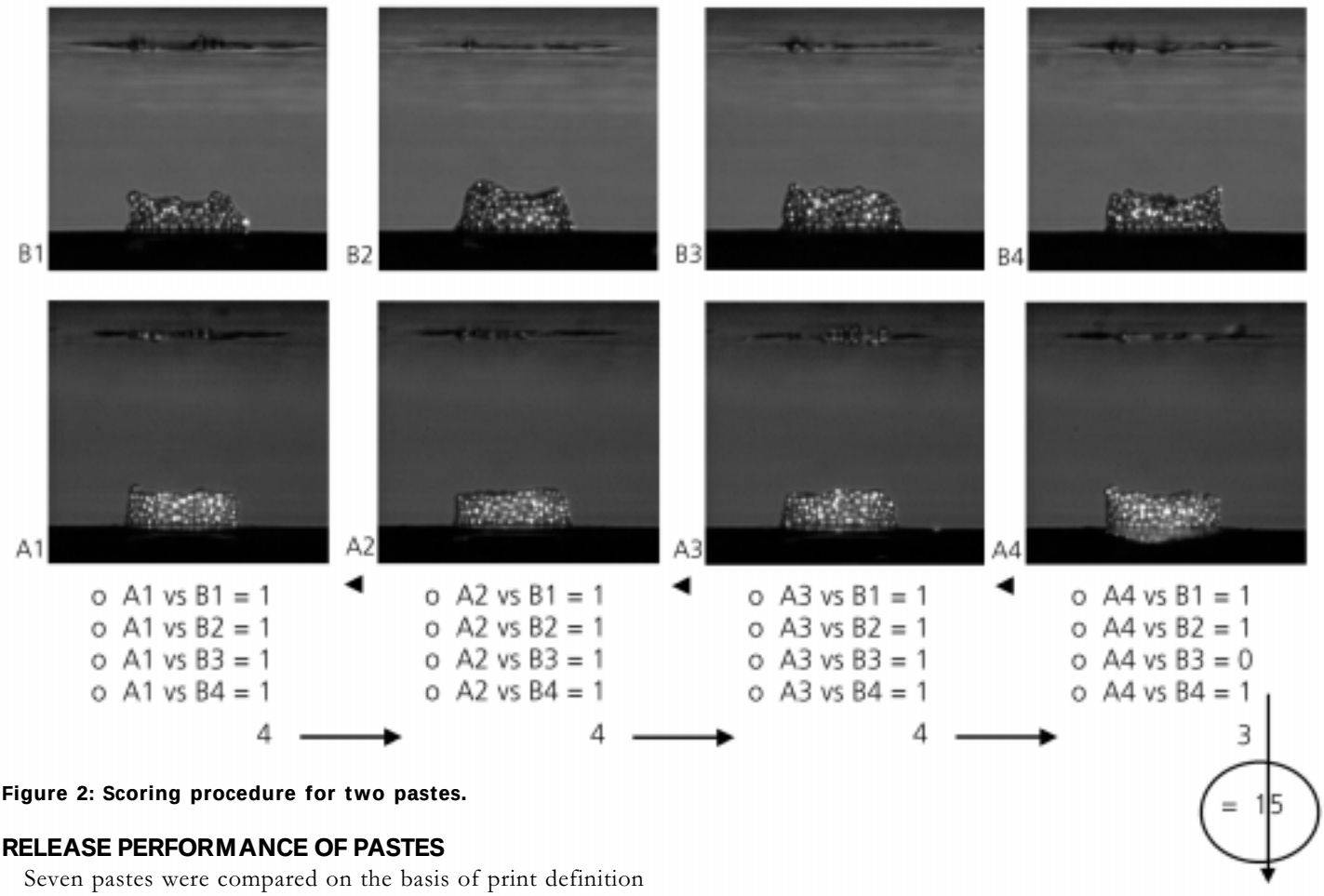

Figure 2: Scoring procedure for two pastes.

RELEASE PERFORMANCE OF PASTES

Seven pastes were compared on the basis of print definition after the release. According to the scoring procedure described above, the relative score between seven pastes ranges between 96 and -96 (6 possible combinations between one paste and the six remaining, with a maximum and minimum score of 16 and -16 per combination).

A summary of paste release performance is shown in Table 1. The scores displayed in the table indicate that we can separate the pastes into four groups: good, medium good, medium poor, and poor performers. It is interesting to note that a paste performance is aperture size dependent. For example, a paste that performs well with large apertures may not release as well from smaller apertures. The case can be illustrated with Paste D, that releases quite well from 20 mil diameter apertures while scoring poorly when used in conjunction with 10 mil diameter apertures.

Shown in Figures 3 and 4 are examples of release sequences to illustrate the comparison between a good (Figure 3) and poor (Figure 4) release. In the release sequences, the stencil and focal plane intersect is shown with the upper dashed line, while the substrate/focal plane intersect is indicated with the lower solid line.

Rank	0.025" diam	0.020" diam	0.015" diam	.010" diam
1	Paste A (54)	Paste D (48)	Paste A (23)	Paste C (46)
2	Paste B (29)	Paste A (29)	Paste C (6)	Paste B (42)
3	Paste C (26)	Paste B (13)	Paste F (2,-23)	Paste G (26)
4	Paste D (14)	Paste E (-13)	Paste G (0)	Paste F (-13,10)
5	Paste E (-9)	Paste C (-19)	Paste B (-1)	Paste E (-31)
6	Paste F (-24,-32)	Paste F (-19,-18)	Paste D (-11)	Paste A (-35)
7	Paste G (-78)	Paste G (-38)	Paste E (-19)	Paste D (-35)

Table 1: Release performance of 7 solder pastes for various aperture diameters (max/min score: 96/-96).

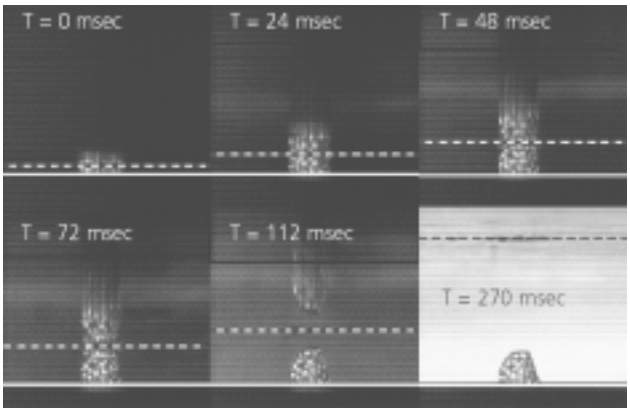

Figure 3: Sequence of real time paste releases from 10 mil diameter round aperture, laser cut 6 mil thick stencil with Paste C.

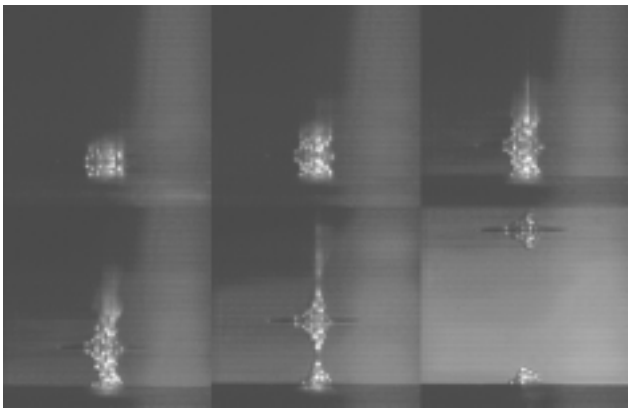

Figure 4: Sequence of real time paste releases from 10 mil diameter round aperture, laser cut 6 mil thick stencil Paste D.

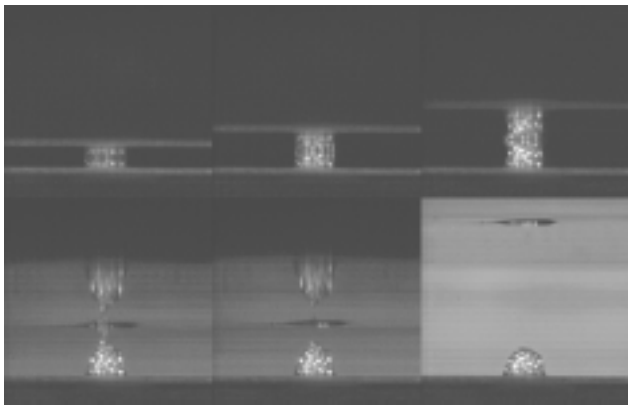

Figure 5: Sequence of paste releases from 10 mil diameter round aperture, electroformed 6 mil thick stencil with Paste C.

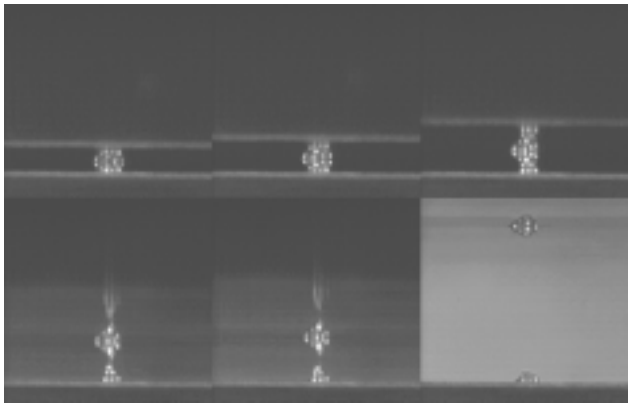

Figure 6: Sequence of paste releases from 10 mil round aperture, chemical etched 6 mil thick stencil with Paste C.

RELEASE PERFORMANCE OF STENCILS

Three stencil manufacturing techniques were compared on the basis of release performance. Composing the test matrix were one chemical etched, one electroformed, and two laser cut stencils (from two manufacturers). Since the test matrix is composed of four elements, the maximum and minimum scores achievable are 48 and -48 respectively. Two sets of experiments were performed independently using different solder pastes (Paste C and D). Results of the tests are summarized in Table 2. Illustrations of typical good and poor releases for the cases of an electroformed and chemical etched stencil are shown in Figures 5 and 6, respectively.

Table 2 clearly shows that electroformed stencils are very good performers regardless of the paste used. Laser-cut stencils are occasionally good performers, in some instances they even tie the electroformed stencils (see laser-cut A vs. E-formed stencil in the case of Paste D). Not all laser-cut stencils are created equal. As can be seen from the second part of Table 2, laser-cut stencils from different manufacturers perform very differently. In general chemical-etched stencils score very poorly, at least for the range of apertures studies here. It is believed that this is caused by the hourglass shape of the apertures, typically produced by the chemical etching process that hinders the full release of the paste from the apertures.

		Ranking / Aperture Geometry							
Stencil	**Paste**	**25 mil**	**Taper (°)**	**20 mil**	**Taper (°)**	**15 mil**	**Taper (°)**	**10 mil**	**Taper (°)**
Electroformed	Paste C	21	3.3	32	3.8	36	3.3	38	3.3
Laser Cut (A)	Paste C	4	3.3	7	2.9	20	2.9	12	3.8
Laser Cut (B)	Paste C	-4	0.5	-21	1.0	-19	1.0	-2	0.5
Chemical Etched	Paste C	-21	1.4	-18	1	-37	2.9	-48	1.4
Electroformed	Paste D	24	3.3	21	3.8	27	3.3	40	3.3
Laser Cut (A)	Paste D	26	3.3	24	2.9	12	2.9	12	3.8
Laser Cut (B)	Paste D	-21	0.5	-2	1.0	-8	1.0	-12	0.5
Chemical Etched	Paste D	-28	(1.4)	-43	(1.0)	-31	(2.9)	-40	(1.4)

Table 2: Release performance of 4 different stencils for various aperture diameters (max/min score: 48/-48).

MODEL OF THE RELEASE MECHANISM

Prediction Technique

A model describing the release process from small stencil apertures has been developed. The model is based on work previously done by Rodriguez et al. [2], with the added feature of taking into account aperture wall taper. The model simulates a step-by-step release of the stencil from the substrate as shown in the Figure 7.

At each step the solder paste shears along an angle of maximum stress θ which ultimately is used to calculate the total volume of paste transferred from the stencil to the substrate. The accuracy of the simulation depends on the size of the steps. Clearly, the larger the steps the less accurate the prediction becomes. Conversely, one may not take arbitrarily small steps for the sake of efficiency and computational overhead. Various simulations were performed using a range of step sizes. The largest step size yielding a converging predicted deposited volume was used for the rest of the simulations.

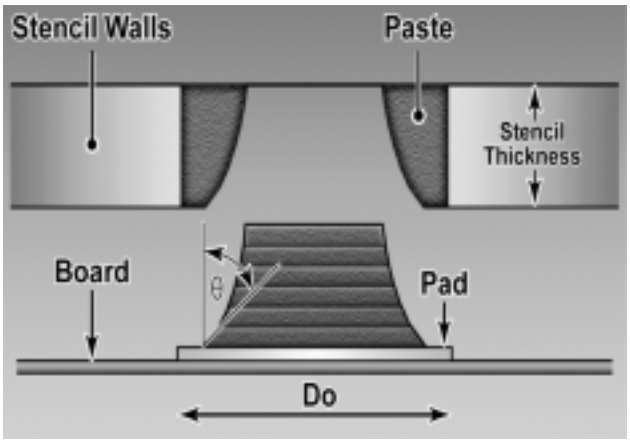

Figure 7: Schematic of paste release mechanism.

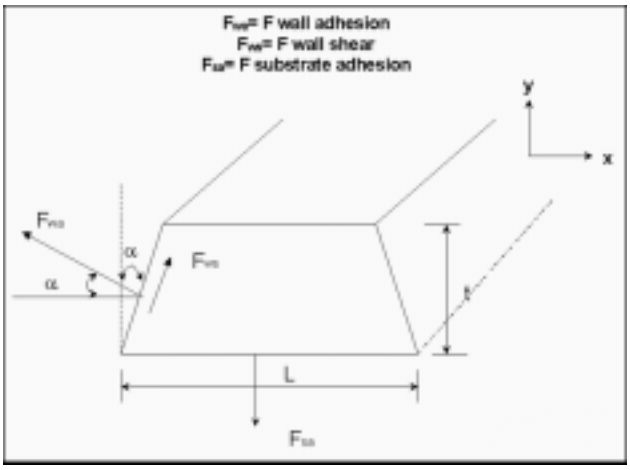

Figure 8: Nomenclature for paste release model.

Figure 8 shows a summary of the forces acting on the solder paste during the release. As the stencil starts to lift, some of the paste remains in the apertures because of the adhesion (F_{wa}) and shear (F_{ws}) forces at the aperture walls. At the same time, the paste is held in contact with the substrate due to adhesion forces (F_{sa}). For the sake of argument let us assume that the taper is nil ($\alpha = 0$). In this case, the release mechanism is simply driven by the force of adhesion at the substrate (F_{sa}) and the shear force at the wall of the aperture (F_{ws}). A simple balance of forces yields:

$$\tau_{ws} * \text{wetted wall area} = \sigma_{sa} * \text{wetted pad area} \quad (1)$$

where t_{ws} is the shear stress caused by shear near the aperture walls, and σ_{sa} is the adhesion force acting normal to the substrate surface.

Using the transformation of stresses, the maximum shear angle θ_{shear} can be obtained for the general case of non-zero taper:

$$\tan(2\theta_{shear}) = \frac{\sigma_x - \sigma_y}{\tau_{xy}} = \frac{-(\sigma_{wa}\sin\alpha + \sigma_{sa})/2}{\tau_{ws}\cos\alpha} \quad (2)$$

where σ_x and σ_y are the normal stresses acting in the x and y direction on an element of paste shown in Figure 9. τ_{xy} represents the shear stress acting in the xy plane.

Equation (1) can be rearranged:

$$\frac{\tau_{ws}}{\sigma_{sa}} = \frac{\text{wetted pad area}}{\text{wetted wall area}} \quad (3)$$

Considering the case where the aperture taper equals zero, then Equation 2 becomes:

$$\tan(2\theta_{shear}) = \frac{\sigma_{sa}/2}{\tau_{ws}} \quad (4)$$

Using Equations 3 and 4, we can determine the plane angle along which maximum shear is achieved in terms of the pad area and wall area.

$$\tan(2\theta_{shear}) = \frac{\text{Wetted wall area}/2}{\text{Wetted pad area}} \quad (5)$$

The model assumes that the paste starts to detach from the stencil one average particle size away from the stencil wall [2]. The initial wetted diameter of the solder paste remaining on the substrate pad is estimated by:

$$D_1 = D_0 - 2*(\text{Average particle diameter}) \quad (6)$$

For subsequent steps the diameter of the deposit at step i is:

$$D_{i+1} = D_i - (2*\Delta t*\tan\theta_{shear}) \quad (7)$$

$$t_{i+1} = t_i - \Delta t \quad (8)$$

The stepping procedure is repeated until the stencil thickness is reached or the deposit diameter becomes zero. The simulations discussed in this paper used a thickness step of 0.01 in. The average particle diameter was taken as 1.375 mils for type 3 pastes and 0.785 mils or type 5 pastes.

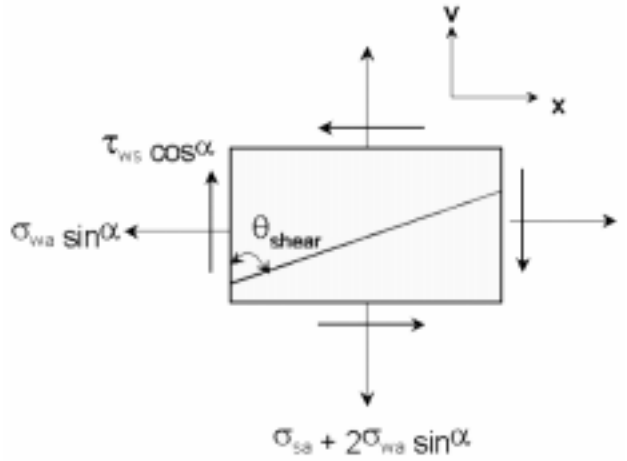

Figure 9: Normal and shear stress diagram for an elemental volume of paste.

Experimental Procedure

Print experiments were performed to validate the model described in this paper. The experiments consisted of printing with three stencil thicknesses (4, 5 and 6 mils), two solder paste types (type 3 and 5), two basic aperture geometries (round and square), and four basic aperture sizes (15, 10, 8 and 6 mils). The elements composing the experimental matrix of interest in this study are summarized in Tables 3-5. One must note that the stencil apertures were designed so that for each round aperture, a square aperture with an equivalent volume was available. This was done for the purpose of determining the aperture geometry that is most efficient at transferring solder from stencil to substrate while keeping the body forces constant.

Stencil Printer Experiment

A modified MPM TF100 printer with a metal squeegee at a print angle of 50 degrees and print speed of 1.5 in./sec was used for the experiment. A down force of 5 lbs was applied to the squeegee. The stencil was lifted with a constant speed of 0.1 in./sec. Print samples were done on bare copper boards. Type 3 and Type 5 63Sn/37Pb solder pastes with 89.9% metal content were selected for the experiment. The experiments are conducted in a controlled environment, i.e. the temperature was maintained at 80F. Thirty boards were printed per experiment.

Measuring Equipment

Solder paste volume measurements were made with a GSI Lumonics 8200 (2x active scanner). A precision/tolerance ratio was conducted, and the gage was found acceptable for the study. The response factors were the release or transfer efficiencies defined as the volume of paste transferred from the stencil to the substrate normalized by the measured volume of the aperture.

Experimental Results and Predictions

Solder paste volume measurements are shown in Figures 10 and 11 for the two paste types selected for this study. Superimposed on the experimental data are the predictions produced from the model developed in this study. The error bars shown in the two figures are representative of the standard 15% error associated with the measuring technique. Clearly, as volumes get smaller, the measurement errors should grow to the point where the technique becomes inadequate. However, this fact has not been shown in either of the figures below.

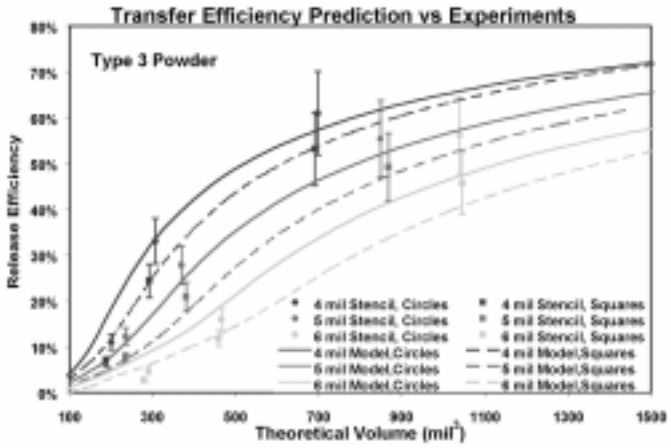

Figure 10: Release efficiency predictions and experiments for Type 3 paste, various stencil thickness and aperture geometry.

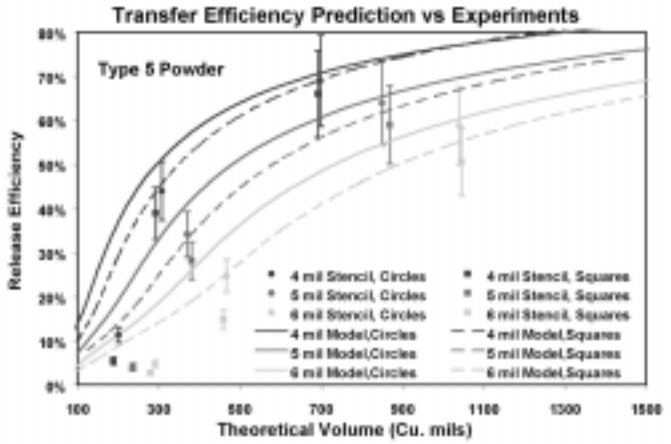

Figure 11: Release efficiency predictions and experiments for Type 5 paste, various stencil thickness and aperture geometry.

Good agreement between predictions and experiment can be observed down to volumes of the order of 300 to 500 cubic mils. The agreement is more pronounced for the thinner stencils and tends to be less accurate for thicker stencils (6 mils) and smaller apertures. As expected, both model and experiment show that release efficiencies are higher for thinner stencils, and that round apertures tend to have better release performances than the square apertures. This observation is consistent with results of a previous study [2]. For small apertures (volumes < 300 cubic mils), the predictions tend to overestimate transfer efficiencies. It is also quite possible that the measurement technique used is grossly inaccurate in this range of volumes.

PASTE FLOW INTO APERTURE STUDY

Model of Pastes Flow in a Squeegee System

In an effort to better understand the issues associated with paste filling stencil apertures, a computational fluid dynamic simulation of the paste flow upstream of a squeegee was performed. Since paste flow measurements are difficult to produce, validation of the predicted flow patterns could not be done by direct comparison to experimental data. It was however possible to verify that the predicted flow fields were consistent with flow patterns observed empirically. Paste flow was simulated through solutions of the two-dimensional governing momentum conservation equations (Navier-Stokes). The non-Newtonian behavior of the paste was modeled along the lines described by Lapasin et al. [3]. In this formulation, the shear rate τ is a function of the shear strain rate $\dot{\gamma}$:

$$\tau^{1/2} = (\eta_\infty \dot{\gamma})^{1/2} + \{\tau_y [1 - \exp(-\alpha\dot{\gamma})]\}^{1/2} \qquad (9)$$

The above was implemented in the calculations as an effective viscosity, the magnitude of which was calculated at each point in the computational domain:

$$\mu = \frac{\tau}{\dot{\gamma}} \qquad (10)$$

$$\mu = \eta_\infty \quad as \quad \dot{\gamma} \to 0 \qquad (11)$$

The following values were used in the above formula:

$$\tau_y = 280 \quad N/m^2$$

$$\eta_\infty = 5.05 \quad N.sec/m^2$$

$$\alpha = 2.55 \quad N.sec$$

The squeegee was taken to travel at 2 in/sec. The density of paste was taken as 5gm/cm3.

The simulation of the squeegee system is shown in Figure 12, where the velocity of selected particles in the computational domain is represented by vectors whose lengths are proportional to the particles' speed. One may notice that the flow of paste predicted by the simulation is consistent with flow patterns observed in practice. This gives credibility to both the flow model and the paste physical properties used for the simulations.

It can also be seen from the simulation that very strong velocity gradients are present just above the stencil (the vectors go from red to blue in a short distance). This probably shear thins the paste that is just above the stencil and assists in driving the paste into the stencil apertures.

Specified Dimension (mil)	Measured Dimension (mil)	Theoretical Volume (mil3)	Measured Volume (mil3)	Percentage Deviation (%)
Circle - 15.00	Circle - 15.0	707	698	1
Square -13.29 x 13.29	Square -13.2 x 13.3	707	691	2
Circle - 10.00	Circle - 10.0	314	307	2
Square - 8.86 x 8.86	Square - 8.7 x 8.6	314	292	0
Circle - 8.00	Circle - 8.1	201	201	7
Square - 7.09 x 7.09	Square - 7.0 x 6.9	201	188	2
Circle - 6.00	Circle - 6.0	113	110	3
Square - 5.32 x 5.32	Square - 5.2 x 5.1	113	103	9

Table 3: Measured aperture dimensions for 4 mil thick stencil

Specified Dimension (mil)	Measured Dimension (mil)	Theoretical Volume (mil3)	Measured Volume (mil3)	Percentage Deviation (%)
Circle - 15.00	Circle - 15.0	884	849	4
Square -13.29 x 13.29	Square -13.8 x 13.6	884	868	2
Circle - 10.00	Circle - 10.0	393	370	6
Square - 8.86 x 8.8 Square - 9.2 x 8.9		393	381	3
Circle - 8.00	Circle - 8.1	251	236	6
Square - 7.09 x 7.09	Square - 7.4 x 7.1	251	235	7
Circle - 6.00	Circle - 6.1	141	130	8
Square - 5.32 x 5.32	Square - 5.3 x 5.2	141	123	13

Table 4: Measured aperture dimensions for 5 mil thick stencil

Specified Dimension (mil)	Measured Dimension (mil)	Theoretical Volume (mil3)	Measured Volume (mil3)	Percentage Deviation (%)
Circle - 15.00	Circle - 15.3	1060	1040	2
Square -13.29 x 13.29	Square -13.7 x 13.8	1060	1045	1
Circle - 10.00	Circle - 10.3	471	467	1
Square - 8.86 x 8.86	Square - 9.2 x 9.2	471	459	3
Circle - 8.00	Circle - 8.3	302	291	4
Square - 7.09 x 7.09	Square - 7.1 x 7.3	302	279	7
Circle - 6.00	Circle - 6.3	170	162	5
Square - 5.32 x 5.32	Square - 5.5 x 5.4	170	147	13

Table 5: Measured aperture dimensions for 6 mil thick stencil

Figure 13 shows a pressure distribution along the length of the stencil, produced mainly by the squeegee traveling at a constant speed on the stencil. Position zero corresponds to where the squeegee meets the stencil. The "bead" of solder paste was assumed to be about 2.3 cm. It can be noticed that very little pressure is generated for about 3/4 of the bead thickness, while the pressure increases sharply as the pastes gets close to the point where the squeegee meets the stencil.

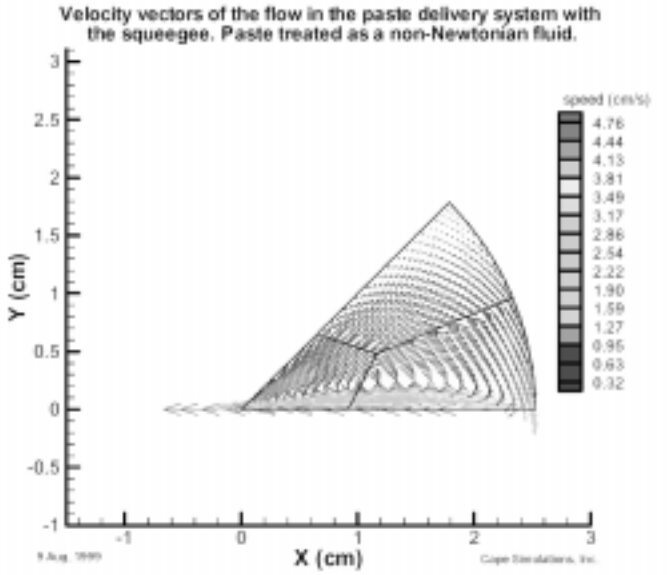

Figure 12: Paste flow simulation for a squeegee system.

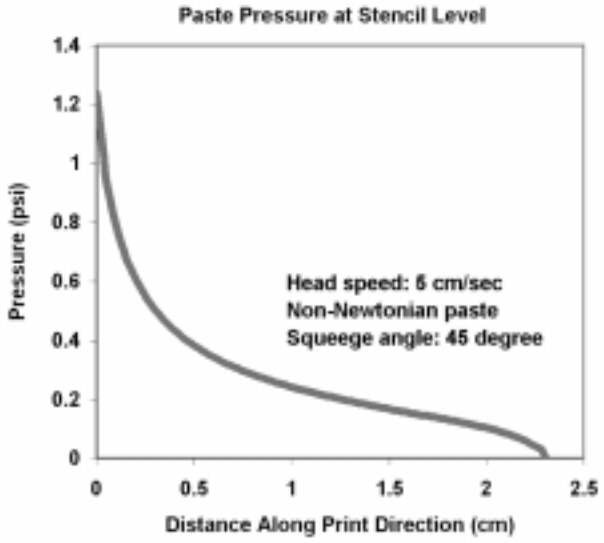

Figure 13: Pressure distribution at stencil level.

Visualization of Paste Flow into Apertures

The visualization platform shown in Figure 1 was slightly modified to visualize paste flowing into apertures. This was done by designing a stencil in which apertures had at least one wall consisting of a small beam splitter cube. This allowed for both lighting and optical access into the aperture cavity.

Figure 14 shows a sequence of pictures acquired using this unique visualization technique. For this particular sequence, the print parameters were as follows:

- Paste: type III, no clean
- Aperture width: 25 mils
- Blade: trailing edge polyurethane (90°)
- Blade speed: 1.5 in/sec
- Blade down force: 1.5 lbs/in of blade

The last picture of the sequence shows the outline of the stencil aperture in rectangles below the squeegee which is shown in diaganol dashed line. In the sequence, the squeegee travels from right to left. Time 0 was taken arbitrarily when the paste starts to flow into the aperture but continues to flow out of the aperture, as can be seen in the first frame of the sequence. In this frame solder particles are in focus at the right of the aperture, which implies a reduced local velocity, while particles are blurred on the left side of the aperture due to their higher relative velocity.

In the next few frames, it can be seen that more and more solder particles achieve zero velocity relative to the stencil and that more paste fills the aperture. Starting at time 206 msec, the paste begins to accelerate because the squeegee approaches the aperture. This acceleration can be seen in the top right corner of the frame. The last three frames illustrate the squeegee severing the excess paste above the aperture.

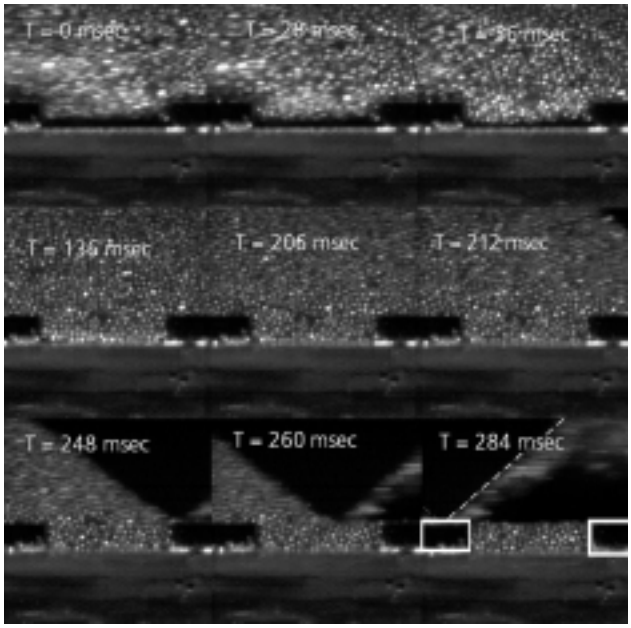

Figure 14: Sequence of paste flowing into a 0.025" wide aperture.

It is interesting to notice from the sequence of Figure 14 that before the paste completely fills the aperture, it spends a significant time traveling with the squeegee in a direction parallel to the stencil. Additionally, some of the solder particles entering the aperture from the right exit the aperture from the left. This is somewhat contrary to the accepted belief of a paste "roll" being the only flow pattern present during the print operation. If only a roll existed during the print, the

only particle motion an aperture would "see" during the fill would primarily be from top to bottom. This is clearly not the case shown by the visualizations.

The aperture starts to fill about 300 msec before the squeegee reached the aperture. This combined with a squeegee speed of 1.5 in/sec, implies that the apertures starts to fill about 0.45" upstream of the point where the squeegee contacts the stencil. This is consistent with the profile shown in Figure 13, where it can be noticed that sufficient pressure has to be produced at the stencil (about 0.2 psi) before paste can be driven into the aperture. The sharp increase in pressure produced closer to the squeegee certainly contributes to the final paste "packing" effect. This appears to happen at about 0.2" upstream of the squeegee, where the local pressure above the stencil is of the order of 0.4 psi.

CONCLUSIONS

A visualization technique has been developed for the real time capture of solder paste transferring from stencils onto substrates and solder paste flowing into stencil apertures during the print operation. Paste releases have been examined for a variety of stencils, stencil aperture sizes, and solder pastes. A semi-quantitative ranking technique has been described. Seven commercially available pastes and three stencil forming techniques have been ranked according to their release performance. Groups of better releasing pastes can be determined. These groups are a function of aperture size. Electroformed stencils are the best performers in terms of transfer efficiency. In some instances, laser-machined stencils perform as well as the E-formed stencils. The chemical etched stencils were found to be poor performers in general.

A model of the partial release of solder paste from various stencils, stencil aperture sizes and geometries, and paste types has been developed. Good agreement is observed between the predictions and experiments down to volumes on the order of 300 to 500 cu mils. For smaller volumes, it is suspected that the model fails and that the measuring technique may be inadequate.

Visualization of solder paste filling an aperture during the print operation has been demonstrated and discussed. A model predicting the paste flow in a squeegee system has been described. The predicted flow field is consistent with empirical evidence. The pressure produced in the paste just above the stencil by the squeegee motion is consistent with the observed time it takes for paste to fill an aperture.

REFERENCES

1. Clouthier, R., "SMT Printing Process for Fine Pitch and Ultrafine Pitch", Proceedings of Surface Mount International Conference, August 1997, pp. 674-683.
2. Rodriguez, G., Baldwin, D., "Analysis of Solder Paste Release in Fine Pitch Printing Processes", ASME Transactions Journal of Electronic Packaging, Vol. 121, September 1999.
3. Lapasin, R., et al., "Visco-elastic Properties of Solder Pastes", Journal of Electronic Materials, Vol. 27, No. 3, 1998.

First published in the proceedings of the 2002 SMTA Boston Advanced Technology Symposium *(June 11-12, Boston, MA).*

BIOGRAPHY

Dr. Gerald Pham-Van-Diep is the director of advanced developments at Cookson Electronics Equipment (Franklin, MA).

Frank Andres is a research engineer at Cookson Electronics Equipment.

Srinivasa Aravamudhan is an intern from SUNY Binghamton (Binghamton, NY).